Design and Experimental Evaluation of EBG-Based Full-Duplex Antennas for 400 MHz Amateur Bands

Hadi Hosseini[2], Adewale K. Oladeinde[1], Suresh Srinivasan[2], Ehsan Aryafar[2], and Bart Massey[2]
[1]Department of Electrical and Computer Engineering, Portland State University, Portland, OR, USA
[2]Department of Computer Science , Portland State University, Portland, OR, USA

***Abstract*—This paper proposes a full-duplex (FD) antenna design with passive self-interference (SI) suppression for the 425 MHz (70 cm) amateur band. The reduction in SI is achieved through using separate transmit (Tx) and receive (Rx) antennas and embedding Electromagnetic Band Gap structures (EBGs) in between the antennas. The antennas are composed of patches made of copper taped over dielectric material, which also contains EBGs. We present the design, optimization, and prototyping of unit antenna elements, EBGs, and integration of EBGs in between the antenna elements. We also evaluate the design through both HFSS (High Frequency Structure Simulator) and over-the-air (OTA) measurements in an anechoic chamber as well as an indoor environment. Through extensive evaluations, we show that (i) antennas can provide over 10 MHz of bandwidth with less than -8 dB return loss and (ii) EBGs can provide up to 42 dB in SI isolation. We also found that there is noticeable gap between HFSS-based simulated SI reduction values and the measured OTA ones, with simulations showing higher SI reduction values than what we could achieve through OTA measurements. We believe that prototyping errors, non-uniformity in the decay value of the board, and OTA coupling between the antennas (in addition to surface current) contribute to discrepancies between simulations and measurements.**

I. Introduction

Full-Duplex (FD) wireless has recently emerged as a new technology that can double the spectral efficiency of next generation wireless networks. A radio with FD functionality can transmit and receive wireless signals at the same time and on the same frequency band. The key challenge to achieving FD is self-interference (SI), in which the transmit (Tx) antenna on the wireless device causes significant interference to its own receive (Rx) antenna. Initial FD radio designs and prototypes where presented in 2010 [1]–[3] and proved the feasibility of building FD radios. Since then, the community has proposed many FD radio designs with different tradeoffs in terms of SI cancellation level, cost, and scalability to MIMO, among others (for a survey refer to [4]). Existing FD radio designs are either limited to 2-6 GHz or mmWave frequency bands.

Our goal in this paper is to study the potential for FD in the 425 MHz amateur band. The 70 cm band, including 425 MHz, is used across a wide set of applications in the amateur radio community, including: (i) Repeaters and FM voice communications, (ii) Digital modes such as D-STAR and DMR digital voice modes and amateur radio mesh networks such as AREDN (Amateur Radio Emergency Data Network), (ii) Amateur satellite communications, (iv) Amateur television transmissions, and (iv) Emergency communications.

Our specific angle to reduce SI as part of amateur FD radio design is to explore antenna design as an avenue to reduce SI. In particular, we investigate the use of electromagnetic band gaps (EBGs) to reduce SI. EBGs are repetitive structure that create a band stop in between Tx and Rx antennas. While our team and other in the community (e.g., [5], [6]) have studied EBG-based FD antenna design for higher frequency sub-6 GHz and mmWave bands, there is no such antenna designs for sub-1 GHz amateur bands. Our key contributions can be summarized as follows:

- **Design:** We present the design steps for a unit patch antenna, EBGs, and integration of EBGs between antennas. We discuss the theoretical modeling and design of EBGs, which provide us with initial estimates of EBG dimensions and structures. We then refine the initial design with extensive Ansys HFSS (High Frequency Structure Simulator) simulations to provide a desirable balance between different objectives such as return loss, frequency bandwidth, SI reduction, and antenna gain.
- **Evaluation:** We clearly discuss the steps we took to fabricate our antennas, so that others in the amateur radio community can replicate our results. We also conduct extensive evaluations of our designs through both HFSS simulations and measurements of a prototype. Specifically, we conduct extensive over-the-air (OTA) measurements of our antennas both inside and outside an anechoic chamber. Our results showed a noticeable gap between simulated and measured SI reduction values, with simulations suggesting more than 60 dB reduction in SI with EBGs, while OTA measurements showed up to 42 dB reduction in SI. We also showed that without EBGs, our antennas provide 30-35 dB reduction in SI depending on the environment[1]. We believe that a combination of prototyping and manufacturing limitations and errors, non-uniformity in the decay value of the board, and especially OTA reflections and coupling (in addition to surface currents) contribute to the difference between simulations and real-world measurements.

The rest of this paper is organized as follows. We describe the related work and background on FD wireless and EBGs in Section II. Next, we discuss our antenna design and prototyping process in Section III. We present the testing and

[1]Note that antenna separation alone reduces SI by about 15 dB based on the path loss formula.

evaluation of our antenna designs in Section IV. Finally, we conclude the paper in Section V.

II. Related Work

In this section, we provide a brief background to FD wireless radio design and EBGs. We also discuss some of the related work in these areas.

A. Full-Duplex Radio Design

Consider a small handheld device or a femto cell with 20 dBm transmission power and noise floor around -93 dBm. To enable FD, one would need to cancel 20+93=113 dBm of SI. This large amount of SI can be removed over multiple stages, namely antenna, analog, and digital cancellation. Fig. 1 depicts how different SI cancellation blocks can be incorporated in the design of a typical radio to enable FD.

Antenna cancellation is a primarily passive SI cancellation technique that arranges Tx and Rx antennas and/or uses RF elements such as reflectors, absorbers, frequency selective surface structures, or EBGs to reduce SI. A common strategy here is to use separate Tx and Rx antennas to benefit from path loss and then use other methods (e.g., extra antennas) for additive SI gains [2], [3], [7]–[12]. In the 425 MHz amateur band, OTA path loss due to antenna separation is about 15 dB with 32.5 cm antenna separation used in our design. Similarly, the work in [13] uses a defected ground structure (DGS) in the ground plane and a MT-30 absorber on top of the array to achieve a high isolation. In another work [14], a 16 dB isolation was achieved by developing a diamond shaped decoupling network with two inverted-F antennas. In [15], a decoupling structure has been introduced that employs parasitic element to emit orthogonal polarized fields to nullify the coupling field around a Rx antenna in a collinear FD dipole array, bringing the total isolation to 50 dB. Furthermore, other literature have explored the use of cross-polarization between a transmitting and receiving antenna elements. For example, [16] and [17] have demonstrated that up to 10 dB of isolation can be achieved with cross polarization. Cross polarization can be combined with other antenna cancellation techniques for additive/additional SI reduction gains.

Analog cancellation is an active cancellation technique that requires knowledge of the SI channel to create a copy of the SI signal in the RF domain and cancel it before the signal is digitized [1], [18], [19]. *Digital Cancellation* is another active cancellation technique that requires knowledge of the SI channel to recreate digital samples of the transmitted signal in the digital domain and subtract them from received samples to remove remaining SI that cannot be removed through antenna and analog cancellation [1].

The work studied in this paper falls in the category of antenna cancellation. Moreover, to the best of our knowledge, we are the first work to study FD antenna design for the 400 MHz amateur band.

B. Electromagnetic Band Gaps

An electromagnetic band gap (EBG) is a phenomenon in which certain materials or structures exhibit a range of frequencies within which electromagnetic waves are prohibited from propagating. Essentially, it creates a band of frequencies where electromagnetic waves, such as radio waves or microwaves, cannot travel through the material or structure. EBGs are typically engineered using periodic structures, such as arrays of conducting elements or dielectric materials arranged in a specific pattern. These structures interfere with the propagation of electromagnetic waves by creating constructive and destructive interference patterns, resulting in band gaps where waves are forbidden to propagate. EBGs have gained widespreadd use in a a variety of applications such as antenna design, microstrip circuits, metamaterials, and photonic crystals, among others [20]–[22]. A useful list of EBG applications for antenna engineering is given in [23].

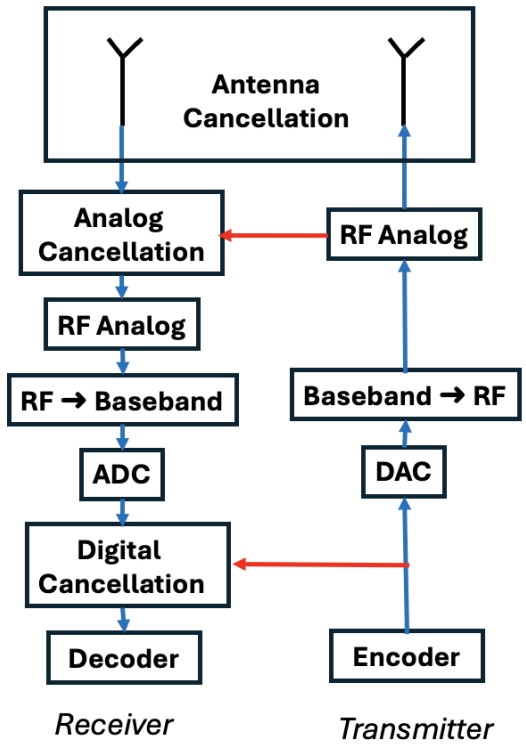

Fig. 1: **In a FD radio, SI is cancelled over multiple stages, including antenna, analog, and digital cancellation. Antenna cancellation refers to a plurality of techniques including use of RF absorbers, reflectors, EBGs, or even additional antennas to reduce SI in the antenna domain.**

EBGs have been used in the related work to reduce mutual coupling. For example, in [21] EBGs have been used to provide an isolation of 14 dB in 28 GHz band as compared to non-EBG design. Further, additional reduction in coupling is achieved by placing hair-pin DGS on the ground plane, resulting in maximum isolation of 48 dB [22]. In other work [24] and [25], EBGs have been used to simultaneously miniaturize the antennas and reduce the mutual coupling in Sub-6 GHz frequency bands. Similarly, [26] proposed a compact EBG design at 60 GHz and showed that (i) the design has a maximum of 30 dB reduction in mutual coupling with 200 MHz isolation bandwidth, and (ii) the size of the proposed EBG unit cell structure is 78% less than conventional uniplanar EBG and 72% less than uniplanar-compact EBG (UC-EBG)

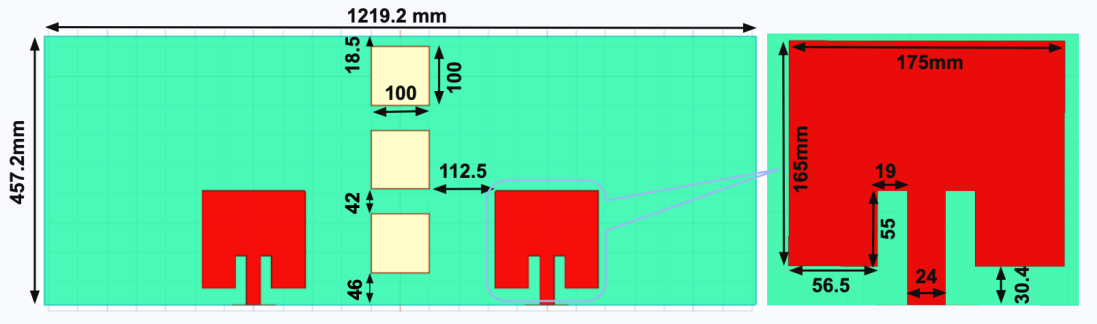

Fig. 2: **Initial design of the full-duplex patch antennas and EBGs.**

operating at same frequency [27]. It is also claimed that the proposed EBG has 12% more size reduction than any other planar EBG structures at microwave frequencies. Further, [28] used a combination of EBGs and choke structure to improve the Tx and Rx isolation of X-band large antenna arrays by 30 dB within a 3% bandwidth in the radar operation band. The achieved isolation and its associated bandwidth are due to a combination of using thicker substrate material and choke structures. In our prior work [5], [6], [29], we discussed EBG-based antenna designs to reduce SI but those design were specific to the 28 GHz mmWave band. In this work, we study the potential for EBG-based SI cancellation over 425 MHz amateur band.

III. Antenna Design and Prototyping Process

In this section, we first discuss the overall design approach, focusing on the objectives, requirements, and constraints that shape the antenna development process. This is followed by an explanation of the design methodology, detailing the use of simulation tools and optimization techniques to achieve the desired performance metrics.

Next, we delve into the prototyping techniques employed to fabricate initial antenna designs, highlighting the materials and methods used to create physical prototypes. Finally, we provide examples of the prototyping process, showcasing notable design iterations and the improvements we achieved.

A. Overview of the Design Approach

Objectives and design requirements. The objective is to design and prototype a full-duplex patch antenna system operating in the Very High Frequency (VHF) band, specifically targeting a resonant frequency of 425 MHz. The system employs one Tx and one Rx element, with an Electromagnetic Band Gap (EBG) structure placed between them to increase isolation between the two antennas. This is critical for mitigating self-interference (SI) and ensuring reliable full-duplex operation. The antenna should exhibit optimal impedance matching with an S11 (return loss) value of -10 dB or lower.

Design constraints. The design is constrained by the physical dimensions of the PCB and the material properties required for optimal antenna performance. Selecting a suitable substrate is critical to ensure that the antenna dimensions align with the operating frequency and propagation requirements for the VHF band. After evaluating various available materials, FR4 was chosen due to its compatibility with the design's size, its dielectric properties ($D_k = 4.4$ and $D_f = 0.016$), and its affordability. These parameters ensure proper impedance matching and maintain compact dimensions suitable for operation in the VHF band. The patch dimensions were calculated based on the resonant frequency of 425 MHz, derived from the standard formula for microstrip patch antennas:

$$L = \frac{c}{2f_r\sqrt{\epsilon_r}}$$

where L is the patch length, c is the speed of light, f_r is the resonant frequency, and ϵ_r is the effective dielectric constant of the substrate. This formula provided a patch length of approximately 175 mm. The width of the patch was optimized to balance the trade-off between bandwidth and radiation efficiency, resulting in a dimension of 165 mm.

The distance between the center of the two antennas was set at 500 mm to minimize mutual coupling and provide adequate isolation, while keeping the design compact. This distance was determined based on HFSS simulations and practical space limitations, ensuring that the EBG structure could effectively suppress coupling. Accurate placement of the Tx, Rx, and EBG structures is crucial to achieving the desired isolation and bandwidth. Additionally, the manual process of taping out the antenna and ground plane with copper tape demands good precision, as even small misalignments can significantly affect resonant frequency, return loss (S11), and isolation (S21).

B. Antenna Design Methodology

Simulation tools and techniques. We utilized Ansys HFSS (High Frequency Structure Simulator) for simulations. HFSS was employed to evaluate return loss (S11), isolation (S21), frequency bandwidth, radiation pattern, and antenna gain. The simulation process involved iterative adjustments to the patch dimensions and EBG structure to enhance isolation and improve bandwidth within the target 423–432 MHz range. For instance, the EBG periodicity was tuned to suppress coupling in the 423–432 MHz range. The patch width was slightly decreased to improve bandwidth while maintaining resonance. The substrate thickness of 12.7 mm was chosen to balance mechanical stability and electrical performance.

Design Framework and Criteria. Fig. 2 illustrates the initial design of the full-duplex patch antenna element and its dimensions in the HFSS environment. The initial design

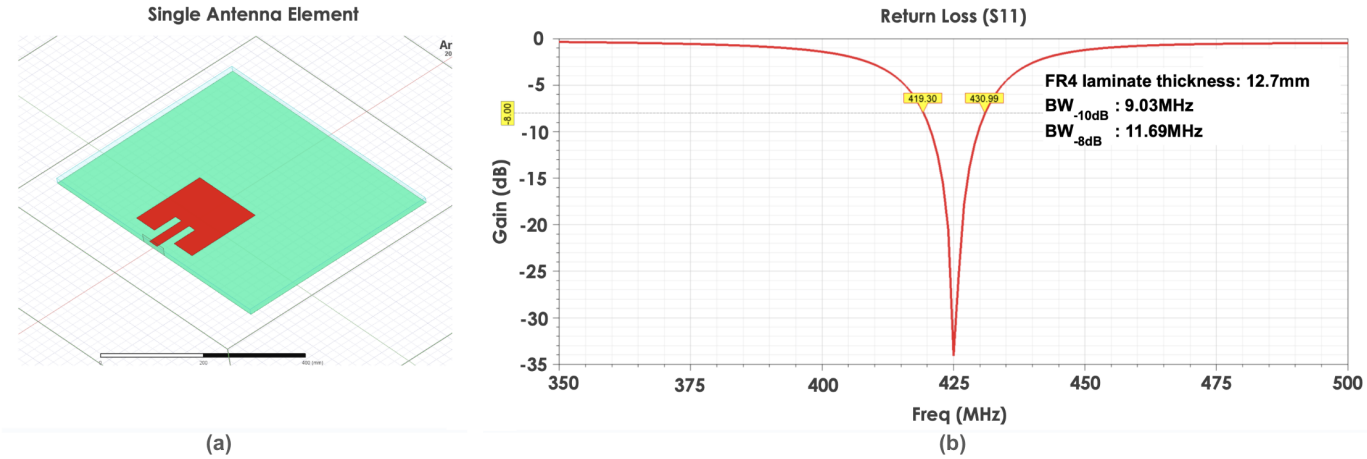

Fig. 3: **(a) Simulated single antenna element in HFSS environment. (b) S-parameter plot showing simulated return loss (S11) and bandwidth for the single antenna element.**

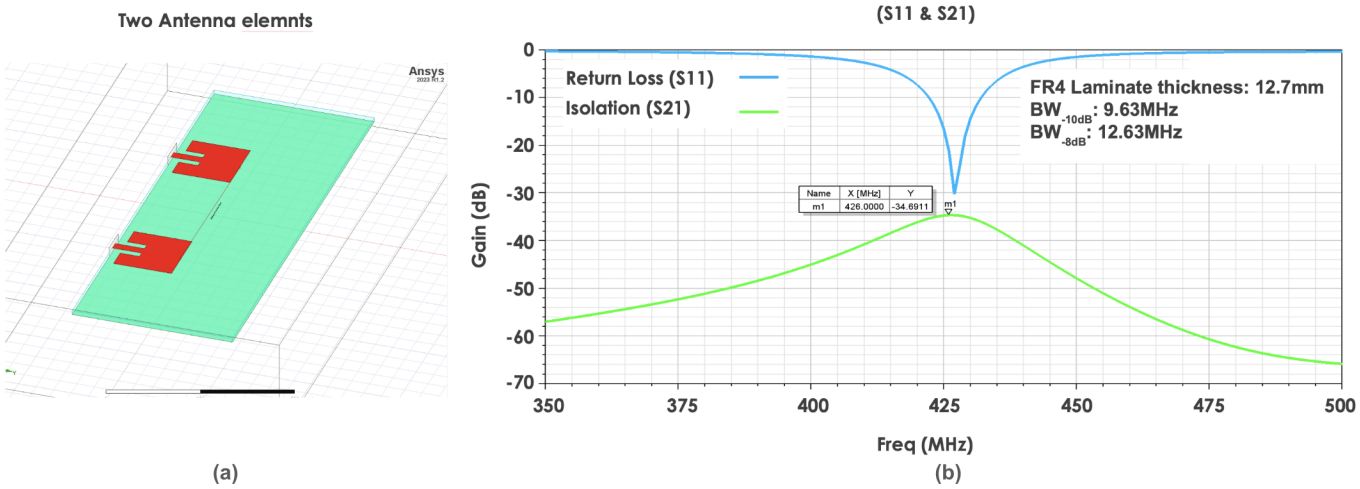

Fig. 4: **(a) Simulated FD antenna with Tx and Rx elements in HFSS environment. (b) S-parameter plots showing simulated return loss (S11) and bandwidth for the single antenna element, and isolation (S21) between two antenna elements after adding second antenna element.**

(Fig. 2) includes symmetric patch antenna elements for Tx and Rx. The EBG structure, represented by yellow squares, was strategically placed to enhance isolation. The substrate panel dimensions were set $18'' \times 48''$ (457.2 mm $\times$ 1219.2 mm) to accommodate the patch elements and EBG structures. Table I illustrates the initial design parameters for the simulation.

TABLE I: **Initial Design Parameters**

Parameter	**Value**
Operating frequency	425 MHz (VHF band)
Target bandwidth	423–432 MHz
Dielectric constant (D_k)	4.4
Loss tangent (D_f)	0.016
FR4 laminate thickness	12.7 mm
Fabrication technique	Copper tape for taping out the antenna
Panel dimensions	18" x 48" (457.2 mm x 1219.2 mm)

Simulation Results. Initial simulations yielded promising results. Fig. 3(a) illustrates the simulated single antenna element in the HFSS environment, while Fig. 3(b) presents the simulated return loss plot as a function of frequency. The target resonance frequency is 425 MHz. At a desired return loss of -10 dB or lower [21], the simulated bandwidth for the single antenna element is 9.03 MHz (420.92–429.95 MHz). For a return loss of -8 dB, the bandwidth increases to 11.69 MHz. Fig. 4(a) illustrates the simulated design of the FD antenna system after the addition of the second antenna element. Fig. 4(b) presents the return loss and isolation after incorporating the second antenna element. The resonance frequency shifts to approximately 427 MHz, with a simulated bandwidth of 9.63 MHz at a return loss of -10 dB. The isolation between the two antenna elements is nearly -35 dB at the target frequency, without EBG integration. Fig. 5(a) shows the simulated FD antenna system in HFSS after adding EBGs. As observed in Fig. 5(b), an isolation of nearly -64 dB is achieved by incorporating EBGs between the Tx and Rx antenna elements. The EBG structures have been refined to meet the target isolation of -50 dB or better. Post-fabrication testing will validate the performance against these simulation results in an indoor environment and an anechoic chamber.

Fig. 6(a) shows a snapshot of the electric field distribution illustrating Tx-Rx mutual coupling without EBG. In Fig. 6(b),

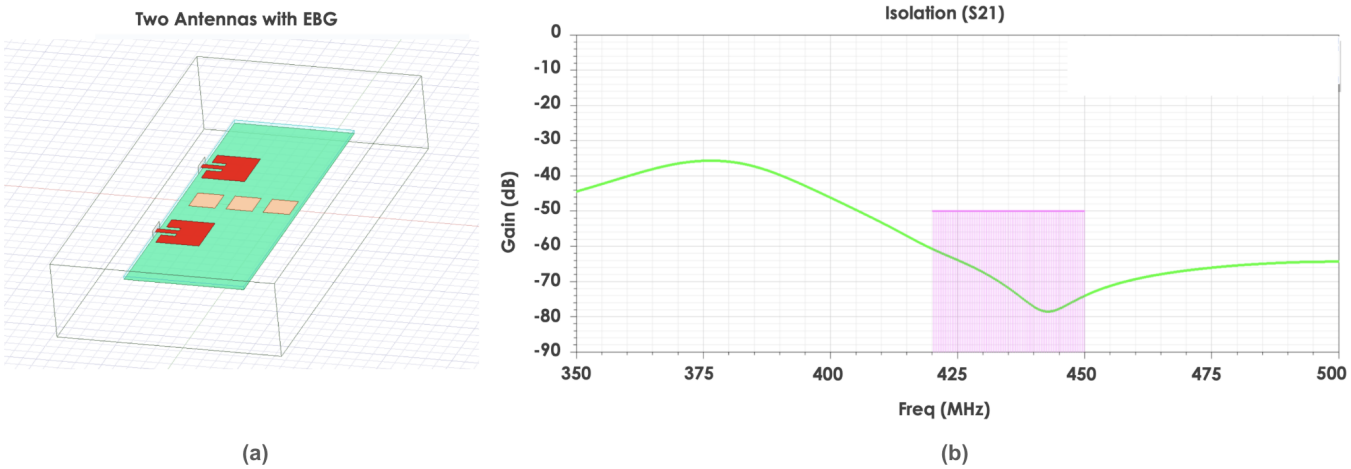

Fig. 5: **(a) Simulated FD antenna with EBGs in HFSS environment. (b) S-parameter plot showing isolation (S21) between two antenna elements after placing EBGs between them.**

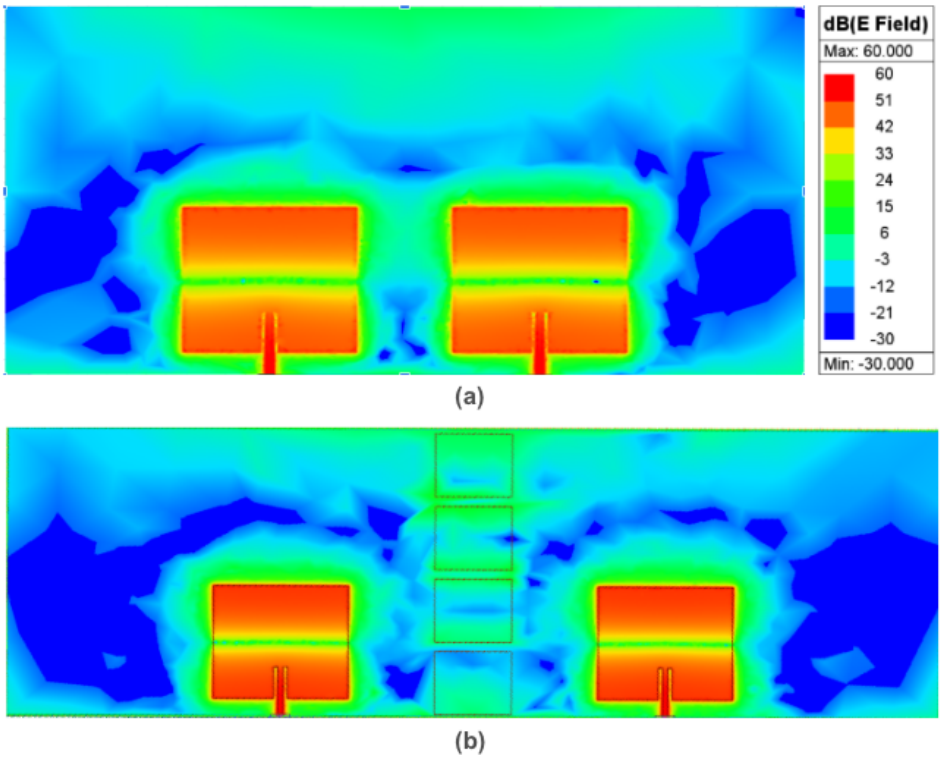

Fig. 6: **(a) A snapshot of the electric field distribution showing Tx-Rx mutual coupling. (b) EBGs create a scattering path within the EBG structure, which reduces the mutual coupling.**

it is observed that the EBGs create a scattering path within the EBG structure, effectively reducing the mutual coupling. Fig. 7(a) illustrates a snapshot of the radiation pattern and coupling effect in an FD communication. Fig. 7(b) shows the simulated 3D radiation pattern of the unit antenna.

Iterative design process and optimization strategies. The simulation process was refined to improve isolation and bandwidth. Adjustments to the EBG periodicity and patch dimensions aimed to enhance coupling suppression. The focus remained on achieving a bandwidth spanning 423–432 MHz, while maintaining high isolation and return loss performance.

C. Prototyping Technique

Fabrication methods. The prototype was fabricated manually by applying copper tape to unclad 18” x 48” x 0.5” FR4 substrate. This involved taping out the patch antenna on the top side of the FR4 material, and covering the back side of the FR4 substrate with copper tape to form the ground plane. FR4 was chosen for its affordability and suitability for operation in the VHF band. (The density and cost of FR4 was not ideal though: the antenna board weighed in at over 13.5 Kg and cost over $400. 1 inch thickness FR4 would have had better electrical properties, but was rejected as impractically heavy

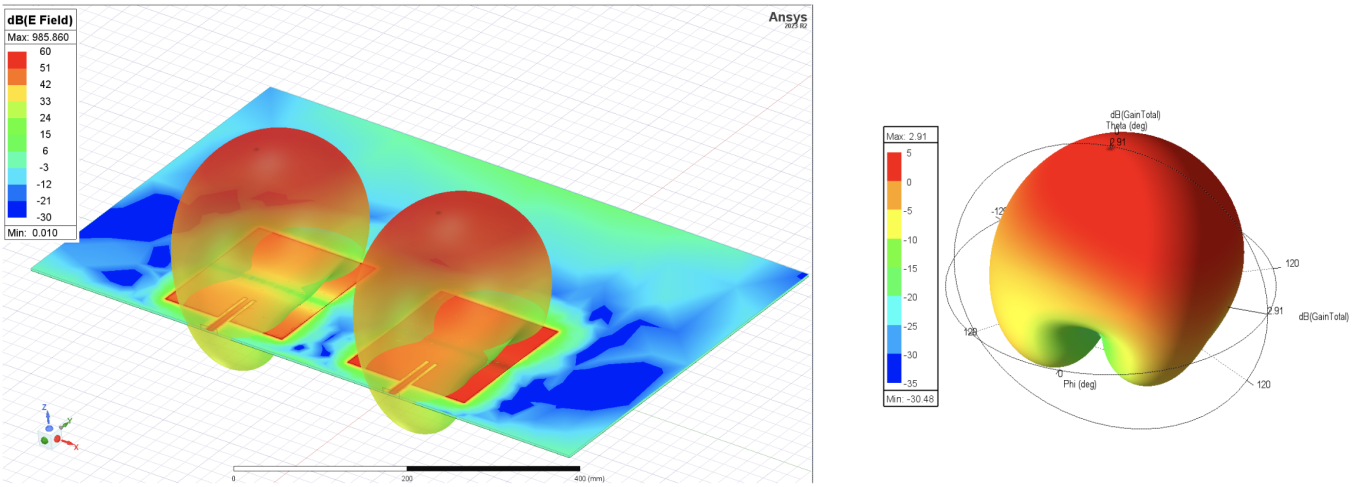

Fig. 7: **(a) A snapshot of the radiation pattern and coupling effect in an FD communication. (b) Simulated 3D radiation pattern of the unit antenna.**

and expensive.) Conductive-adhesive copper tape was selected for its ease of application and conductivity, making it ideal for rapid prototyping.

Challenges in transitioning from design to fabrication. One significant challenge is the manual precision required for taping out the patch antenna and ground plane with copper tape. Even minor misalignments of a few millimeters can significantly impact performance, affecting resonant frequency, return loss (S11), and isolation (S21). Achieving precise alignment during fabrication is critical for ensuring the antenna meets its design specifications.

IV. Evaluation, Testing, and Validation

In this section, we first outline the objectives of the testing phase, emphasizing the key performance metrics that guide the evaluation process. This is followed by a detailed description of the measurement setup and procedures, including the testing environments and equipment used.

Next, we present the results and analyze the performance of the prototypes, comparing measured outcomes to simulated predictions and discussing any observed discrepancies. We then describe the iterative process of refining the design based on test results, addressing performance challenges, and ensuring compliance with specifications. Finally, we summarize the validation of the final prototype, highlighting its readiness for production or deployment.

A. Testing Objectives

Goals of the testing phase. The primary goal of the testing phase is to verify the antenna design's compliance with performance requirements by evaluating key performance metrics. This includes ensuring that the resonant frequency falls within the target range of 423–432 MHz and achieving higher isolation (SI reduction) with the EBG structure. Additionally, the testing aims to verify the return loss and bandwidth for values of -10 dB or lower to ensure proper impedance matching, validate the radiation patterns for both Tx and Rx elements, and measure the antenna gain to confirm alignment with design expectations. The stability of the antenna's performance will also be assessed in various environments, including an indoor environment with multipath and a controlled anechoic chamber environment.

B. Measurement Setup and Procedures

Description of test environments. The evaluation was conducted in two distinct environments:

- *Indoor Testing:* The initial objective was to measure the S-parameters of the unit antenna in an indoor environment, composed of a large lab area. The Vector Network Analyzer (VNA) was calibrated for a frequency range of 360 MHz to 460 MHz. The LiteVNA, a portable vector network analyzer operating from 50 kHz to 6.3 GHz, was used to measure S11 and S21. Its design, based on the NanoVNA and SAA2, provides a compact solution for measuring reflection and transmission coefficients without requiring a bulky analyzer. The LiteVNA employs a single mixer, enabling S11 and S21 measurements via RF switching, as well as TDR/DTF measurements through IFFT calculations.

  Fig. 8(a) shows the single Tx (Rx) antenna taped out on FR4 material using copper tape, while Fig. 8(b) presents the measured return loss for the single antenna element. The x-axis of the VNA plot spans 100 MHz, starting from 360 MHz, with subdivisions of 20 MHz. The y-axis (yellow numbers) is logarithmically scaled at 3 dB per division. At the resonance frequency of 425 MHz, the measured S11 is -17.42 dB, and the bandwidth at -10 dB return loss is approximately 15 MHz.

  Fig. 9(a) illustrates two antenna elements taped out on FR4 material using copper tape. Fig. 9(b) shows the measured S11 for a single antenna after adding the second antenna element, along with the measured S21

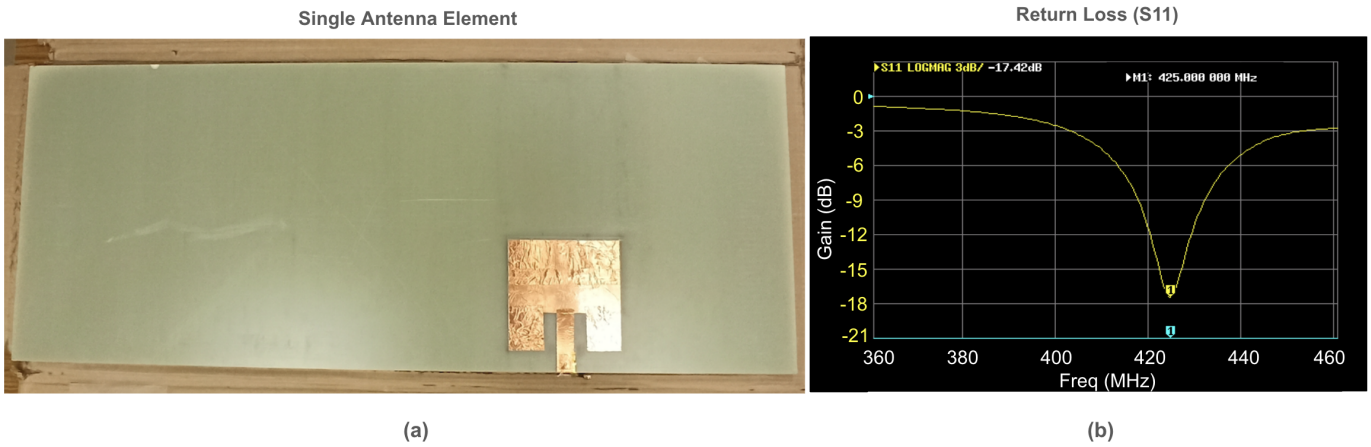

Fig. 8: **(a) Single antenna element taped out on FR4 material using copper tape. (b) Measured indoor return loss (S11) for the fabricated Antenna.**

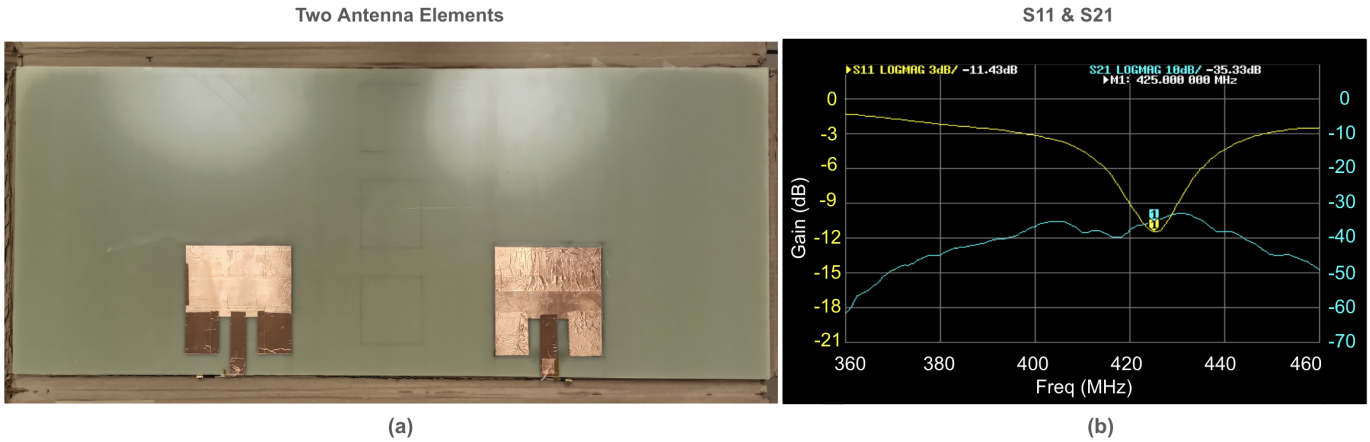

Fig. 9: **(a) Two antenna elements taped out on FR4 material using copper tape. (b) Measured return loss (S11) of a single antenna after adding second antenna element, and isolation (S21) between two antenna elements indoors.**

between the two antenna elements in free space. The y-axis on the left (yellow numbers), scaled at 3 dB per division, represents the S11 gain, while the y-axis on the right (cyan numbers), scaled at 10 dB per division, represents the S21 gain. After adding the second antenna, at the resonance frequency of 425 MHz, the measured S11 is -11.43 dB, with a bandwidth of approximately 9 MHz at -10 dB return loss. The S21 value at the target frequency is -35.33 dB.

Multiple configurations of the EBG structure were tested next and placed between the Tx and Rx antenna elements. Isolation and return loss were measured for various configurations of the EBGs. In partciular, after taping out EBGs we created different configurations through small (e.g., 1 mm) increase or decrease in EBG dimensions to find the configuration with the best performance. Measurements were then taken after applying the EBG structure, with each configuration compared for S11 and S21 parameters. Fig. 10(a) presents the FD antenna system after placing the best EBG structure between the two antenna elements using copper tape. Fig. 10(b) shows the measured return loss of a single antenna and the isolation between the two antenna elements indoor after incorporating the EBGs. After applying the EBGs, at the resonance frequency of 425 MHz, the measured S11 is -12.87 dB, with a bandwidth of approximately 10 MHz at -10 dB return loss. The S21 value at the target frequency is -42.12 dB, indicating that applying EBGs results in an improvement of about 7 dB in the indoor environment.

- *Anechoic Chamber Testing:* Fig. 11(a) shows the equipment and measurement setup used in the anechoic chamber. A Hewlett Packard (8753E) vector network analyzer was employed to measure return loss and isolation in a controlled environment. The FD patch antenna was placed in the chamber using a wooden structure, as depicted in Fig. 11(c), which held the antenna under test (AUT). Fig. 12(a) presents the measured return loss for the unit antenna in the anechoic chamber. At the resonance frequency of 425 MHz, the measured S11 is -16.97 dB, with a bandwidth of approximately 10 MHz at -10 dB return loss. The measured S21 value at the target frequency, without

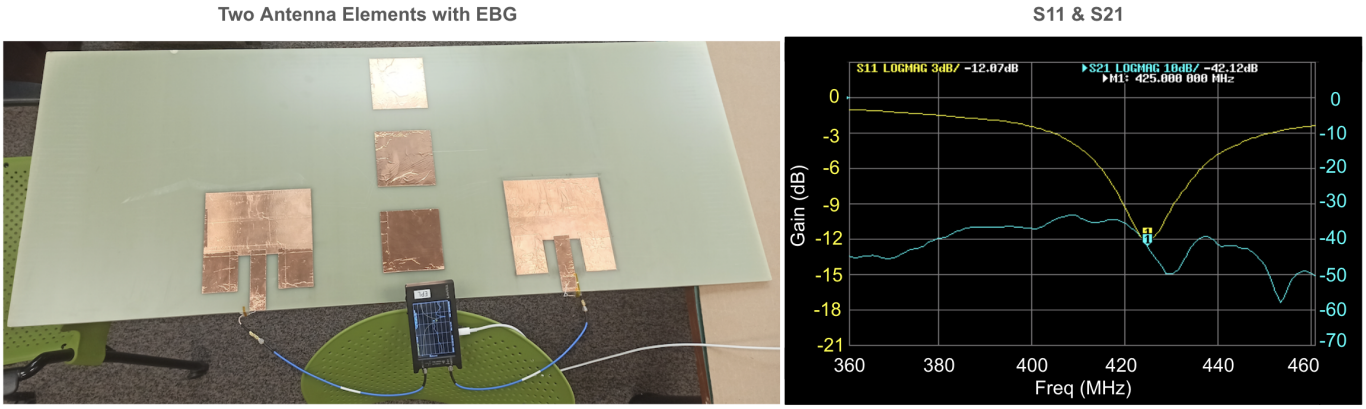

Fig. 10: **(a) Placing EBGs between two antenna elements using copper tape. (b) Measured return loss (S11) of a single antenna and isolation (S21) between two antenna elements indoors after placing EBGs between them.**

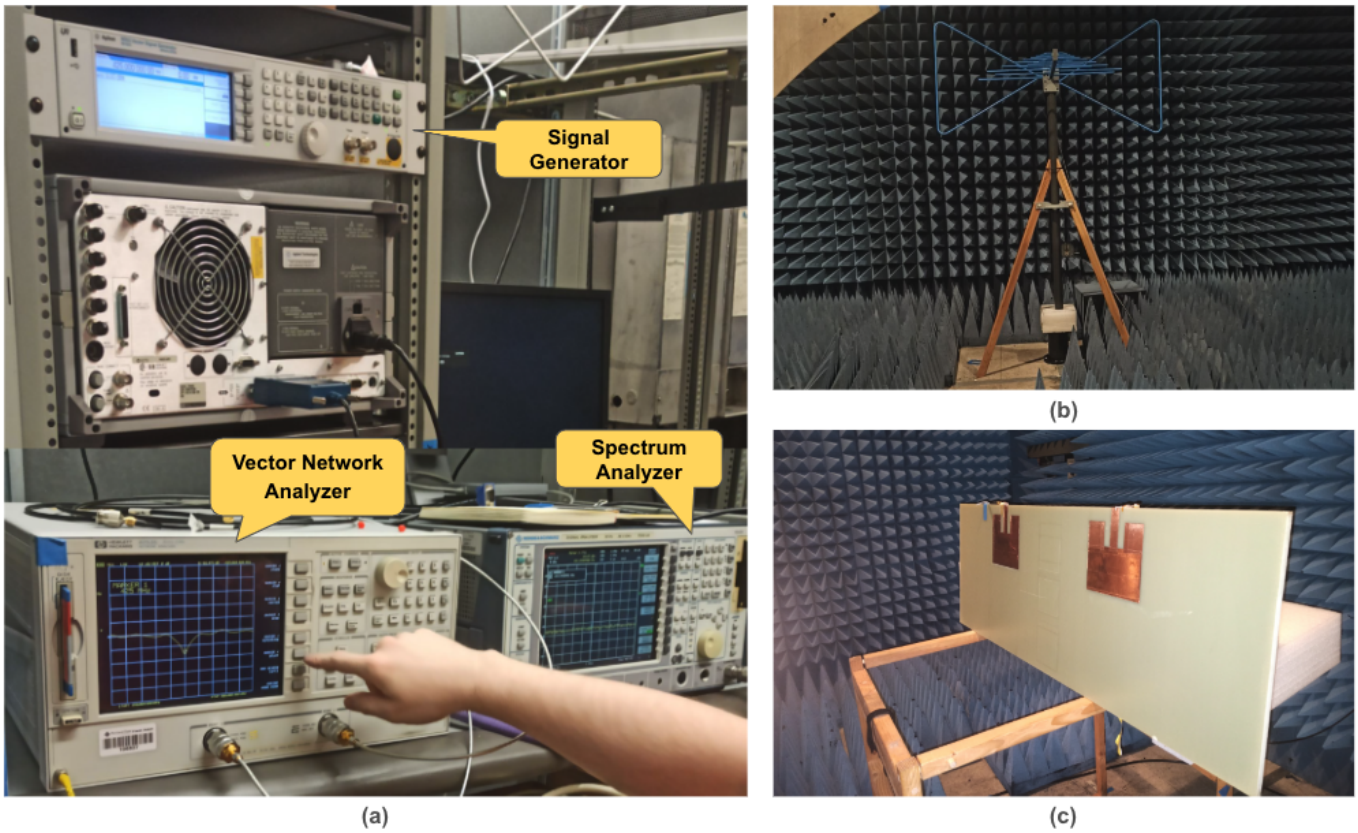

Fig. 11: **(a) Measurement setup in anechoic chamber. (b) Position of the reference antenna (RA) in anechoic chamber. (c) Position of the antenna under test (AUT) in anechoic chamber.**

EBG incorporation, is -30.78 dB, as shown in Fig. 12(b). These measurements validate the return loss and isolation values obtained in both the simulation environment and free space.

Radiation patterns were subsequently measured at the target frequency of 425 MHz. For the far-field measurement setup, a signal generator (Fig. 11(a)) was used to generate a continuous waveform at 425 MHz with 0 dBm power, which was fed into the reference antenna (RA). Antenna gain was evaluated using an RA with a gain of +6 dBm, positioned 350 cm away. The free space path loss at 425 MHz was calculated as 35.98 dB, with cable losses measured at 3.14 dB. The received gain at the AUT was then measured by the spectrum analyzer at the target frequency of 425 MHz. Fig. 11(b) shows the position of the log-periodic antenna used as the RA. Radiation patterns were evaluated horizontally, covering angles from $-45°$ to $+45°$ by rotating the wooden structure and cardboard boxes designed to hold the antenna in the correct position and angle. Fig. 13(a) illustrates the setup used for rotating the antenna, along

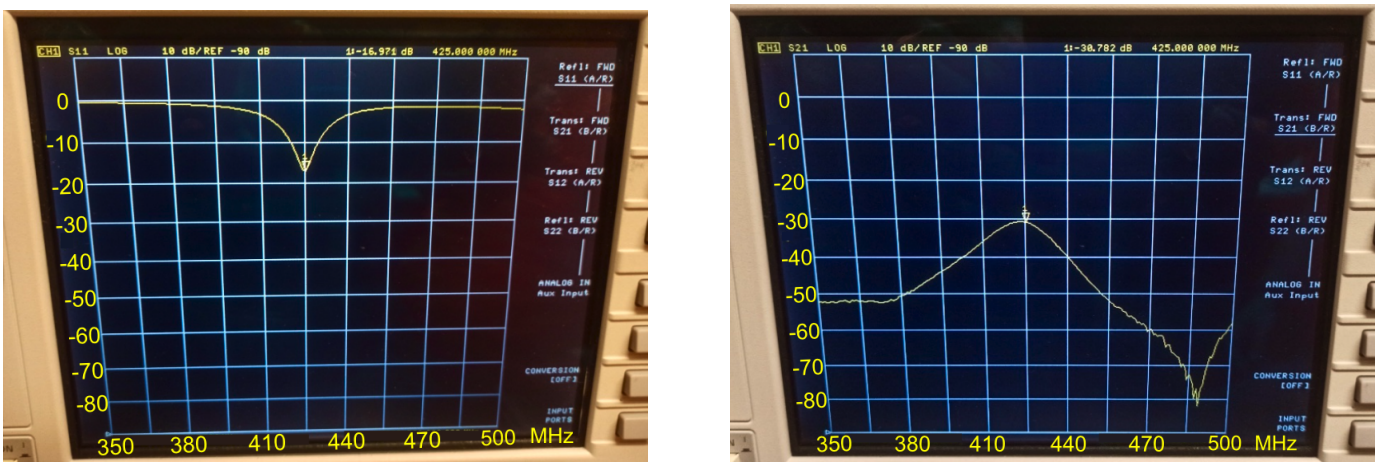

(a) (b)

Fig. 12: **(a) Measured return loss for unit antenna in anechoic chamber. (b) Measured isolation between Tx and Rx antenna elements in chamber.**

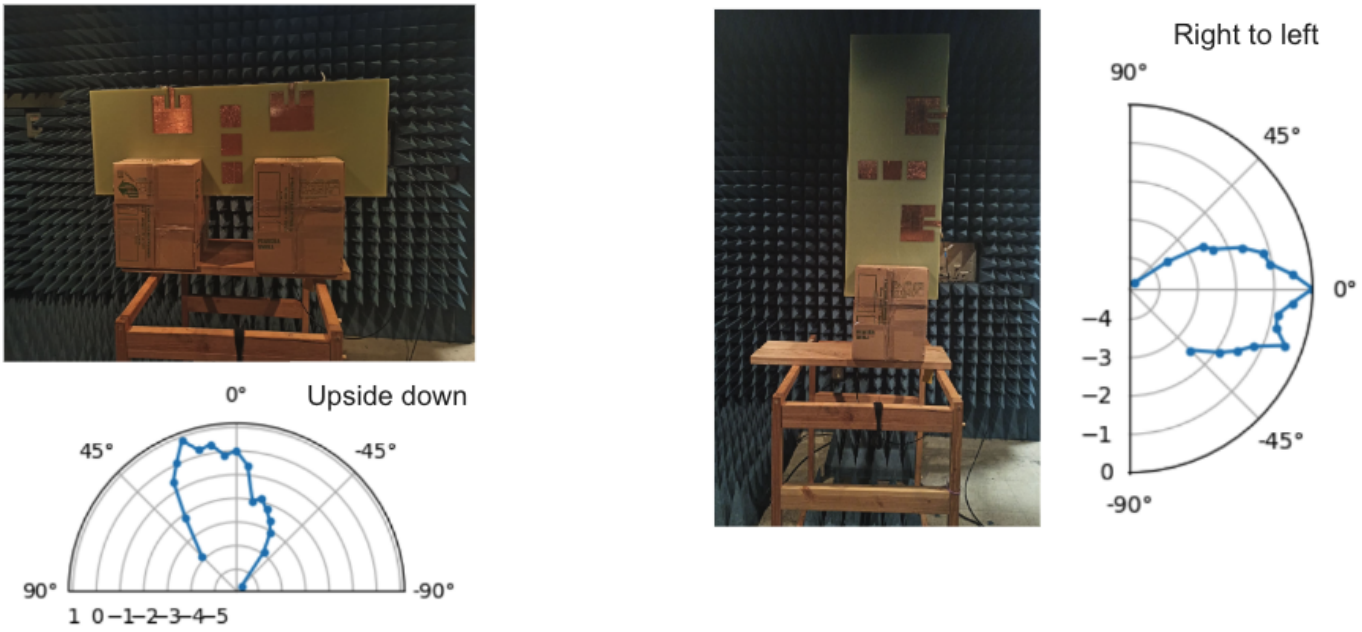

(a) (b)

Fig. 13: **(a) Radiation pattern of the AUT in the azimuth plane (horizontal plane) with the patch antenna positioned upside down. (b) Radiation pattern of the AUT in the azimuth plane (horizontal plane) with the patch antenna positioned right to left.**

with the radiation pattern of the AUT in the azimuth plane (horizontal plane) when the patch antenna is positioned upside down. Fig. 13(b) shows the radiation pattern of the AUT in the azimuth plane when the patch antenna is positioned from right to left.

C. Results and Performance Analysis

Measured vs. simulated results.

Return Loss : S11 for the first antenna before applying the second antenna showed good matching within the design specifications. After integrating the second antenna, minor shifts were observed, which were mitigated by fine-tuning the patch antenna dimensions.

Isolation : Without the EBG structure, isolation values were between -30 dB (in anechoic chamber) and -35 dB (indoors). Adding the EBG improved isolation by about 7 dB (-42 dB indoor). This is, however, lower than more than 60 dB of isolation that we could optimize through HFSS simulations.

Radiation Patterns: Anechoic chamber tests confirmed symmetrical and consistent radiation patterns for both Tx and Rx elements across the measured angles.

Gain and Bandwidth: The antenna system demonstrated a bandwidth efficiency of 9.63 MHz, with gain measurements aligning closely with simulated results.

Impact of environmental factors on performance. Noise Interference: External RF sources and ambient noise impacted isolation measurements. Multipath Reflections: Reflections from nearby objects affected the mutual coupling and radiation pattern measurements. Temperature Effects: Variations in ambient temperature affected the dielectric constant of FR4,

slightly shifting the resonance frequency.

D. Validation and Iterative Improvements

Refinement based on test results. Initial testing revealed that the manual taping process introduced slight misalignments, impacting returrn loss and isolation. This was addressed by refining the taping methodology and recalibrating the system. Further optimization of EBG periodicity improved isolation from -38 dB to the target -42 dB. Adjustments to substrate length and copper tape application enhanced bandwidth and minimized return loss variations.

Strategies for addressing performance discrepancies. Firstly, through a series of measurements in various environments, we identified that noise and environmental factors play a significant role in measurements, especially regarding the isolation parameter. Multipath reflections and over-the-air coupling can greatly affect the level of SI reduction in between the two antenna elements. Secondly, the fabrication method is a critical factor influencing the performance of the FD patch antenna system. Even minor changes in the dimensions of the patch antenna can lead to substantial differences in its performance. Therefore, cutting the copper tape must be done with great precision, as variations of less than one millimeter can significantly alter the S11 and S21 parameters. Utilizing 3D printing techniques can enhance performance and help address discrepancies between simulation results and real-world scenarios. Additionally, material properties and inconsistencies can contribute to discrepancies. In simulations, materials like FR4 are assumed to have uniform dielectric properties (e.g., constant D_k and D_f), but real-world variations in these properties can impact performance. Temperature fluctuations during operation can also alter the material's dielectric constant, leading to shifts in the resonance frequency and reduced efficiency.

Furthermore, connector losses and imperfect soldering can introduce additional signal attenuation and impedance mismatches, especially at higher frequencies. These issues are often underestimated in simulations but become prominent during real-world testing.

Lastly, the modeling assumptions in simulation tools, such as perfectly symmetric and ideal structures, may not capture real-world imperfections like uneven copper application, surface roughness, or asymmetry in the antenna elements. Accounting for these imperfections during design and fabrication can help minimize discrepancies.

V. Conclusion and Future Work

Full-duplex wireless is an important technology, which promises to double the spectral efficiency of the next generation wireless networks. While the majority of the related work has studied FD wireless in higher frequency sub-6 GHz and mmWave bands, this paper studied the potential for FD wireless in the 400 MHz amateur band. Specifically, we studied the use of EBGs as part of antenna design to reduce SI. We showed through HFSS simulations that one can achieve more than 60 dB of SI reduction through integration of EBGs as part of the antenna design. However, our over-the-air measurements of a prototype showed only up to 42 dB of SI reduction. We believe that prototyping errors, non-uniformity in the decay value of the board, and OTA coupling between the antennas (in addition to surface current) contribute to discrepancies between simulations and measurements.

As part of our future work, we plan to extend this work in several way. First, we learned throughput the project that weight and cost of FR4 panels are major obstacles for experimentation particularly for amateur radio users. Thus, we plan to extend the design to use cheaper and lighter material (e.g., foam boards) instead of FR4. Second, we plan to boost the OTA reduction in SI by combining EBGs with other techniques such as RF absorbers or guard strips.

VI. Acknowledgments

This research was supported in part by a grant from Amateur Radio Digital Communications (ARDC).

References

[1] M. Duarte and A. Sabharwal, "Full-Duplex Wireless Communications Using Off-the-shelf Radios: Feasibility and First Results," in *Forty Fourth Asilomar Conference on Signals, Systems and Computers*, November 2010, pp. 1558–1562.

[2] J. I. Choi, M. Jain, K. Srinivasan, P. Levis, and S. Katti, "Achieving Single Channel, Full Duplex Wireless Communication," in *Proceedings of ACM MobiCom*, September 2010.

[3] A. K. Khandani, "Methods for Spatial Multiplexing of Wireless Two-Way Channels," in *US Patent US7817641*, 2010.

[4] Besma Smida, Ashutosh Sabharwal, Gábor Fodor, George C. Alexandropoulos, Himal A. Suraweera, and Chan-Byoung Chae, "Full-Duplex Wireless for 6G: Progress Brings New Opportunities and Challenges," *IEEE Journal on Selected Areas in Communications*, vol. 41, no. 9, pp. 2729–2750, Sept. 2023.

[5] A. K. Oladeinde, E. Aryafar, and B. Pejcinovic, "EBG-Based Self-Interference Cancellation to Enable mmWave Full-Duplex Wireless," in *2021 IEEE Texas Symposium on Wireless and Microwave Circuits and Systems (WMCS)*, 2021.

[6] A. K. Oladeinde, E. Aryafar, and B. Pejcinovic, "EBG Placement Optimization in a Via-Fed Stacked Patch Antenna for Full-Duplex Wireless," in *2022 IEEE-APS Topical Conference on Antennas and Propagation in Wireless Communications (APWC)*, 2022.

[7] H. Yon, N. H. Abd Rahman, M. A. Aris, M. H. Jamaluddin, I. K. Chen Lin, H. Jumaat, F. N. M. Redzwan, and Y. Yamada, "Development of C-Shaped Parasitic MIMO Antennas for Mutual Coupling Reduction," in *Electronics 2021, 10(19), 2431; https://doi.org/10.3390/electronics10192431*, 2021.

[8] X J. Lin, Z. M. Xie, and P. S. Zhang, "Integrated Filtering Microstrip Duplex Antenna Array with High Isolation," in *International Journal of Antennas Propagation. vol. 2017, Article ID 4127943, 8 pages, 2017. https://doi.org/10.1155/2017/4127943*, 2017.

[9] E. Everett, A. Sahai, and A. Sabharwal, "Passive self-interference suppression for full-duplex infrastructure nodes," *IEEE Transactions on Wireless Communications*, vol. 13, no. 2, pp. 680–694, 2014.

[10] W. T. Slingsby and j. P. McGeehan, "Antenna isolation measurements for on-frequency radio repeaters," in *1995 Ninth International Conference on Antennas and Propagation, ICAP '95 (Conf. Publ. No. 407)*, 1995, vol. 1, pp. 239–243 vol.1.

[11] A. Ramos, T. Varum, and J. N. Matos, "A review on mutual coupling reduction techniques in mmwaves structures and massive mimo arrays," *IEEE Access*, vol. 11, pp. 143143–143166, 2023.

[12] E. Aryafar, M. A. Khojastepour, K. Sundaresan, S. Rangarajan, and M. Chiang, "MIDU: Enabling MIMO Full Duplex," in *Proceedings of ACM MobiCom*, 2012.

[13] A. Madni and Wasif W. T. Khan, "Design of a compact 4-element gnss antenna array with high isolation using a defected ground structure (dgs) and a microwave absorber," *IEEE Open Journal of Antennas and Propagation*, vol. 4, pp. 779–791, 2023.

[14] S. W. Cheung D. Wu, Q. L. Li, and T. I. Yuks, "'decoupling using diamond-shaped patterned ground resonator for small mimo antennas," *IET Microwave Antenna and Propagation*, vol. 11, pp. 177–183, 2017.

[15] K. Iwamoto, M. Heino, K. Haneda, and H. Morikawa, "Design of an antenna decoupling structure for an inband full-duplex collinear dipole array," *IEEE Transactions on Antennas and Propagation*, vol. 66, no. 7, pp. 3763–3768, 2018.

[16] H. Nawaz and I. Tekin, "Dual-polarized, differential fed microstrip patch antennas with very high interport isolation for full-duplex communication," *IEEE Transactions on Antennas and Propagation*, vol. 65, no. 12, pp. 7355–7360, 2017.

[17] C.-Y.-D. Sim, C. C. Chang, and J.-S. Row, "Dual-feed dual-polarized patch antenna with low cross polarization and high isolation," *IEEE Transactions on Antennas and Propagation*, vol. 57, no. 10, pp. 3321–3324, 2009.

[18] K. E. Kolodziej, J. G. McMichael, and B. T. Perry, "Multitap RF Canceller for In-Band Full-Duplex Wireless Communications," in *IEEE Transactions of Wireless Communications. Volume: 15, Issue: 6*, June 2016.

[19] E. Aryafar and A. Keshavarz-Haddad, "PAFD: Phased Array Full-Duplex," in *Proceedings of IEEE Infocom*, 2018.

[20] D. M. N. Elsheakh, H. Elsadek, and E. A. Abdallah, "Antenna Designs with Electromagnetic Band Gap Structures," in *Proceedigs of Asia-Pacific Microwave Conference*, May 2012.

[21] F. Yang and Y. Rahmat-Samii, "Microstrip Antennas Integrated with Electromagnetic Band-Gap (EBG) Structures: A Low Mutual coupling Design for Array Applications," in *IEEE Transactions on Antennas and Propagation*, October 2003, pp. 2936–2946.

[22] S. Dey, S. Dey, and S. K. Koul, "Isolation Improvement of MIMO Antenna using Novel EBG and Hair-Pin Shaped DGS at 5G Millimeter Wave Band," in *IEEE Access*, 2021, vol. 9, pp. 162820–162834.

[23] "Electromagnetic Band Gap Structures in Antenna Engineering," Cambridge University Press, 2009.

[24] S. Ghosh, T. N. Tran, and T. Le-Ngoc, "Dual-layer ebg-based miniaturized multi-element antenna for mimo systems," *IEEE Transactions on Antennas and Propagation*, vol. 62, no. 8, pp. 3985–3997, 2014.

[25] H. S. Farahani, M. Veysi, M. Kamyab, and A. Tadjalli, "Mutual coupling reduction in patch antenna arrays using a uc-ebg superstrate," *IEEE Antennas and Wireless Propagation Letters*, vol. 9, pp. 57–59, 2010.

[26] Mu'ath J. Al-Hasan, Tayeb A. Denidni, and Abdel Razik Sebak, "Millimeter-wave compact ebg structure for mutual coupling reduction applications," *IEEE Transactions on Antennas and Propagation*, vol. 63, no. 2, pp. 823–828, 2015.

[27] Antti E. I. Lamminen, Antti R. Vimpari, and Jussi Saily, "Uc-ebg on ltcc for 60-ghz frequency band antenna applications," *IEEE Transactions on Antennas and Propagation*, vol. 57, no. 10, pp. 2904–2912, 2009.

[28] Lei Qiu, Fei Zhao, Ke Xiao, Shun-Lian Chai, and Jun-Jie Mao, "Transmit–receive isolation improvement of antenna arrays by using ebg structures," *IEEE Antennas and Wireless Propagation Letters*, vol. 11, pp. 93–96, 2012.

[29] A. K. Oladeinde, E. Aryafar, and B. Pejcinovic, "MmWave Tx-Rx Self-Interference Suppression through a High Impedance Surface Stacked EBG," in *MDPI Electronics Journal*, 2024.